Catena xxx (2011) xxx–xxx

Contents lists available at ScienceDirect

Catena

journal homepage: www.elsevier.com/locate/catena

Sediment source identification in a semiarid watershed at soil mapping unit scales

F.E. Rhoton [a,*], W.E. Emmerich [b], M.A. Nearing [b], D.S. McChesney [a], J.C. Ritchie [c]

[a] USDA-ARS National Sedimentation Laboratory, Oxford, MS 38655, USA
[b] USDA-ARS Southwest Watershed Research Center, Tucson, AZ 85719, USA
[c] USDA-ARS Hydrology and Remote Sensing Laboratory, Beltsville, MD 20705, USA

ARTICLE INFO

Article history:
Received 1 October 2010
Received in revised form 4 April 2011
Accepted 1 May 2011
Available online xxxx

Keywords:
Enrichment ratios
Parent material
Stable carbon isotopes
Runoff and erosion
Suspended sediment

ABSTRACT

Selective erosion and transport of silt and clay particles from watershed soil surfaces leads to enrichment of suspended sediments by size fractions that are the most effective scavengers of chemical pollutants. Thus, preferential transport of highly reactive size fractions represents a major problem relative to sediment/chemical transport in watersheds, and offsite water quality. The objective of this research was to develop an approach to identify sediment sources at a soil mapping unit scale for the purpose of designing site specific best management practices which affect greater reductions in runoff and erosion losses. Surface soil samples were collected along transects from each of the major 25 mapping units in six subwatersheds of the Walnut Gulch Experimental Watershed. Suspended sediments were collected from supercritical flumes at the mouth of each subwatershed. Laboratory analyses included basic soil/sediment physical and chemical properties, radioisotopes, and stable carbon isotopes, all by standard methods. Aggregation index (AI) values [$100 \cdot (1 - \text{water dispersible clay}/\text{total clay})$] were taken as an indicator of relative soil erodibility. Potential sediment yield index (PSYI) values were calculated by multiplying percent relative area for individual soil mapping units times ($100 - \text{AI}$). Particle size results indicated that suspended sediments were enriched in clay, relative to the watershed soils, by an average of 1.28. Clay enrichment ratios (ER) were significantly ($P \leq 0.01$) and positively correlated with AI, an indication that these two parameters can be equated with erodibility and sediment yield. The PSYI values for the six subwatersheds ranged from 68.0 to 81.7. The stable carbon isotope data for the suspended sediments gave a C3 (shrubs) to C4 plant (grasses) ratio that ranged from 1.06 to 2.25, indicating greater erosion from the more highly erodible, shrub-dominated subwatersheds which also coincided with the highest PSYI values. Correlation coefficients determined individually for PSYI versus clay ER, C3/C4 plant ratios, and multivariate mixing model results were: 0.962 ($P \leq 0.01$), 0.905 ($P \leq 0.01$), and 0.816 ($P \leq 0.05$), respectively. These statistically significant relationships support the accuracy of a potential sediment yield index approach for identifying suspended sediment sources at soil mapping unit scales.

1. Introduction

Estimates of annual, worldwide soil erosion losses published over the past few decades (Brown and Wolf, 1984; Pimentel, 2000; Pimentel et al., 1995; Boardman, 1998; Trimble and Crosson, 2000) vary in some cases by an order of magnitude, however, it is safe to state that the losses, in terms of tonnage and dollar costs, are in the tens of billions. Regardless of the validity of these soil erosion loss estimates, more efficiently designed best management practices (BMP) are needed at relatively small scales to reduce runoff and sediment loads to acceptable levels. This can be accomplished by detailed, comprehensive landscape analysis using soil geomorphology and pedology approaches to characterize soil erodibility from the standpoint of its role in the identification of sediment sources at a range of scales.

In terms of sediment transport and its role in environmental degradation, silt and clay fractions in suspended sediment largely control water quality problems that create impaired waters, both physically by contributing to excessively high turbidity, and chemically through the transport of adsorbed contaminants such as mercury, arsenic, lead, and phosphorus. Enrichment of silt and clay fractions in the suspended sediment (Rhoton et al., 2007) increases with transport distance from the source materials as the coarser, denser fractions are deposited (Slattery and Burt, 1997). Nutrients and heavy metal contaminants are concentrated orders of magnitude above normal soil and water concentrations by this process (Ongley, 1982; Rhoton and Bennett, 2009), because most of the cation exchange capacity is associated with the clay fractions (<2 μm) that are preferentially eroded and transported (Rhoton et al., 1979; Walling and Moorehead, 1989). Further, silt and clay fractions of suspended sediments are enriched in organic carbon relative to the

* Corresponding author. Tel.: +1 662 232 2938; fax: +1 662 232 2988.
E-mail address: fred.rhoton@ars.usda.gov (F.E. Rhoton).

0341-8162/$ – see front matter © 2011 Published by Elsevier B.V.
doi:10.1016/j.catena.2011.05.002

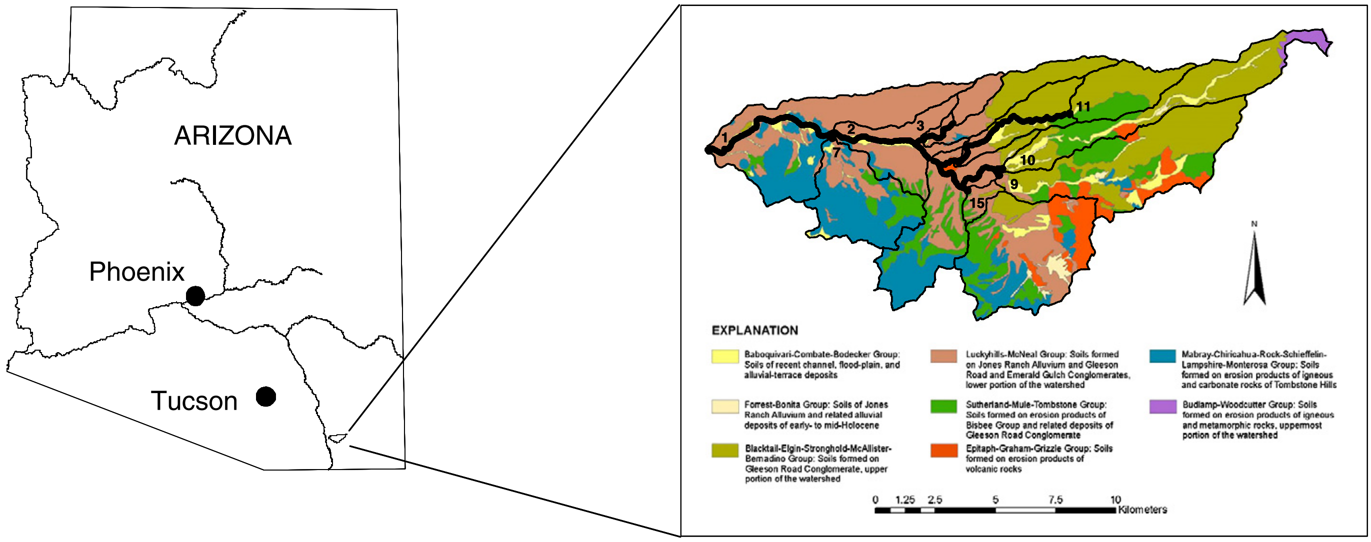

Fig. 1. Map of Walnut Gulch Experimental Watershed, Arizona, showing soil and parent material distributions by subwatershed.

source soils in the watershed (Rhoton et al., 2008). Thus, the eventual deposition of suspended sediments results in organic carbon and nutrient enrichments in reservoir bottom sediments (Avnimelech and McHenry, 1984).

Numerous studies conducted over the past few decades (Caitcheon, 1998; Dearing et al., 1986; Oldfield et al., 1979; Peart and Walling, 1988; Rhoton et al., 2008; Slattery et al., 1995; Walling, 2005; Walling and Woodward, 1992) have addressed the issue of sediment source identification at watershed scales. Within this context, the two primary approaches employed for sediment source identification are direct monitoring and fingerprinting. Direct monitoring uses methods such as erosion pins, runoff troughs, sediment samplers, and grab samples to estimate relative contributions of individual sources to overall sediment loads in a watershed (Sutherland and Bryan, 1989). Sediment fingerprinting relies on companion suspended sediment, streambank, and watershed soil properties, and is the only approach that can be used at large watershed scales to distinguish between sediment source types within or between individual storm events (Slattery et al., 1995).

Recent sediment fingerprinting research introduced a soil geomorphology and pedology component to account for variability in soil properties as a function of surface morphometry factors (Rhoton et al., 2008). Data from this work were used in a multivariate mixing model to estimate individual subwatershed (10^3 ha) contributions to sediment loads transported from the watershed, irrespective of streambank and channel sources. Model results showed that the greatest amount of sediment originated in the subwatersheds with the lowest soil aggregation index (highest erodibility), and the highest clay enrichment ratios (ER) in the suspended sediment. Thus, clay ER in suspended sediment was an accurate indicator of sediment sources at scales smaller than watersheds, with sediment yields increasing

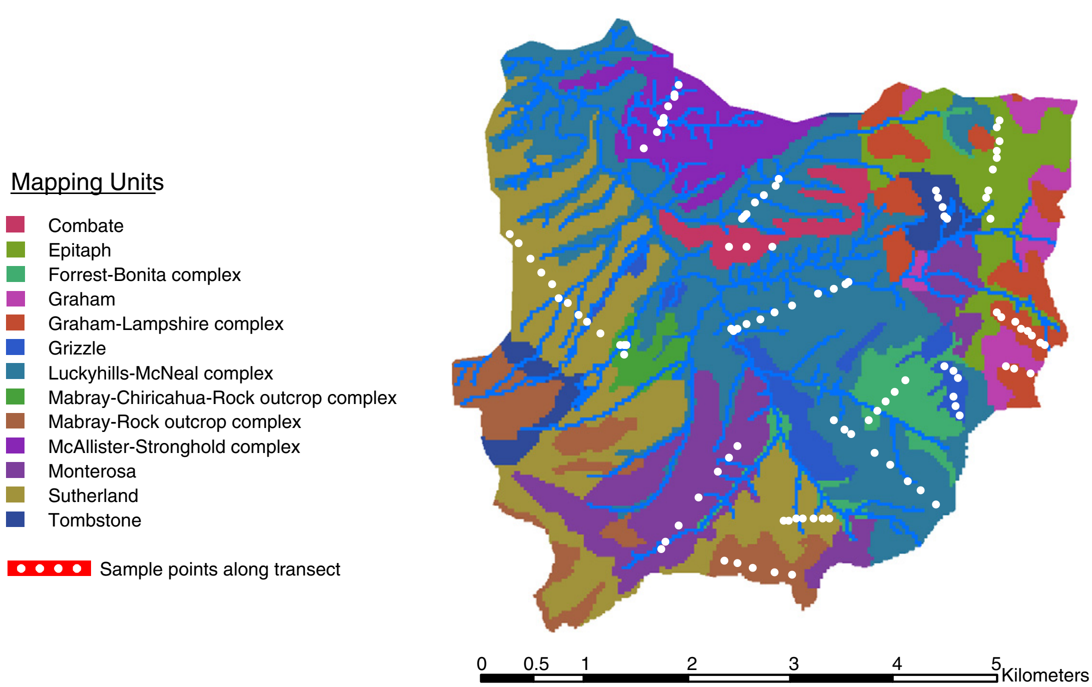

Fig. 2. Watershed soil sampling approach based on relative area of soil mapping units, illustrating sample collection points along individual transects in subwatershed 15.

Table 1
Soil taxonomy and landforms of mapping units in Walnut Gulch Experimental Watershed.

Soil phase	Taxonomic classification	Landform
Baboquivari gravelly coarse sandy loam	Fine-loamy, mixed, thermic Ustic Haplargids	Fan remnant
Bernardino gravelly clay loam	Fine, mixed, superactive, thermic Ustic Calciargids	Fan remnant
Blacktail gravelly sandy loam	Fine, mixed, superactive, Calcidic Agriustolls	Fan remnant
Bodecker extremely gravelly sandy loam	Sandy-skeletal, mixed, thermic Ustic Torriorthents	Flood plains
Bonita cobbly silty clay	Fine, smectitic, thermic Typic Haplotorrerts	Flood plains
Budlamp very gravelly fine sandy loam	Loamy-skeletal, mixed, thermic Lithic Haplustolls	Mountains
Chiricahua very cobbly loam	Clayey, mixed, superactive, thermic, shallow Ustic Haplargids	Hills
Combate gravelly loamy coarse sand	Coarse-loamy, mixed, non-acid, thermic Ustic Torrifluvents	Alluvial fans
Elgin very gravelly fine sandy loam	Fine, mixed, thermic Calcic Paleargids	Fan remnant
Epitaph very cobbly clay loam	Fine, smectitic, thermic Petrocalcic Calcitorrerts	Hills
Forrest loam	Fine, mixed, superactive, thermic Ustic Calciargids	Basin floor
Graham cobbly clay loam	Clayey, smectitic, thermic Lithic Ustic Haplargids	Hills
Grizzle coarse sandy loam	Fine loamy, mixed, superactive, thermic Ustic Calciargids	Hills
Lampshire very cobbly loam	Loamy-skeletal, mixed, superactive, non-acid, thermic Lithic Ustic Torriorthents	Hills
Luckyhills very gravelly sandy loam	Coarse-loamy, mixed, thermic Ustic Haplocalcids	Fan remnant
McAllister loam	Fine-loamy, mixed, thermic Ustic Calciargids	Fan remnant
McNeal gravelly sandy loam	Fine-loamy, mixed, thermic Ustic Calciargids	Fan remnant
Mabray very gravelly loam	Loamy-skeletal, carbonatic, thermic Lithic Ustic Torriorthents	Hills
Monterosa very gravelly sandy loam	Loamy-skeletal, mixed, superactive, thermic, shallow Ustic Petrocalcids	Fan remnant
Mule very gravelly fine sandy loam	Loamy-skeletal, carbonatic, thermic Ustic Haplocalcids	Fan remnant
Schiefflin very stony loamy sand	Mixed, thermic Lithic Torripsamments	hills
Stronghold gravelly fine sandy loam	Coarse-loamy, mixed, thermic Ustic Haplocalcids	Fan remnant
Sutherland gravelly fine sandy loam	Loamy-skeletal, carbonatic, thermic, shallow Calcic Petrocalcids	Fan remnant
Tombstone extremely gravelly fine sandy loam	Loamy-skeletal, mixed, thermic Ustic Haplocalcids	Fan remnant
Woodcutter very gravelly fine sandy loam	Loamy-skeletal, mixed, thermic Lithic Agriustolls	Hills and mountains

with an increase in ER. Rhoton et al. (2008) also reported substantially higher suspended clay concentrations at the watershed outlet, relative to those measured for the subwatersheds. In this case, suspended clay concentrations of the individual subwatersheds closely mirrored their estimated relative contributions to the total suspended sediment load leaving the watershed.

Di Stefano and Ferro (2002) discussed in detail the mechanisms associated with clay enrichment and sediment delivery both at the hillslope and watershed scales. The two basic mechanisms by which sediment becomes enriched in clay are that of preferential erosion of fine particles, usually thought of as taking place at the hillslope scale, and preferential conveyance of fine particles as the sediment is transported to a watershed outlet because of preferential deposition of coarser materials. On a watershed that is relatively homogeneous with respect to soils, and hence with respect to both soil erodibility and preferential erosion of fines from the hillslopes, it is expected that a greater enrichment ratio is indicative of a lower sediment delivery ratio (Walling, 1983; eq. 5) due to preferential conveyance, and hence a lower sediment delivery rate. Where soils are not homogeneous, this assumption may require adjustment. These concepts form the basis of the model of Di Stefano and Ferro (2002) for linking clay enrichment and sediment delivery.

Table 2
Soil mapping unit areas by subwatershed in the Walnut Gulch Experimental Watershed.

	Subwatershed					
Soil mapping unit	3	7	9	10	11	15
	ha					
Baboquivari–Combate complex		19.5	188.7	190.1	6.7	
Blacktail gravelly sandy loam				245.5		
Budlamp–Woodcutter complex				64.6		
Chiricahua very gravelly clay loam		101.3				
Combate loamy sand	3.0	8.2				60.0
Elgin–Stronghold complex	120.2		881.7	283.7	75.3	
Epitaph very cobbly loam			71.9	18.1		152.7
Forrest–Bonita complex			12.6	18.7		103.2
Graham cobbly clay loam			175.7	13.8		66.8
Graham–Lampshire complex			122.1	9.1		113.4
Grizzle coarse sandy loam						81.6
Lampshire–Rock outcrop complex		28.4	52.5			
Luckyhills loamy sand		14.0	7.0			
Luckyhills–McNeal complex	443.4	286.8	44.6	1.1		740.1
Mabray–Chiricahua–Rock outcrop complex		295.8				36.3
Mabray–Rock outcrop complex		193.4				150.7
McAllister–Stronghold complex	273.0		317.4	229.3	61.4	144.8
Monterosa very gravelly fine sandy loam	12.7	15.6				248.6
Riverwash–Bodecker complex		8.1		12.6		
Schiefflin very stony loamy sand		190.2				
Stronghold–Bernadino complex	94.9		38.6	178.8	421.1	
Sutherland–Mule complex		65.7				
Sutherland very gravelly fine sandy loam		141.2				403.9
Tombstone very gravelly fine sandy loam			486.3	252.0	223.6	73.4
Woodcutter gravelly sandy loam				61.9		
Totals	947.2	1368.1	2398.9	1579.4	788.2	2375.6

Please cite this article as: Rhoton, F.E., et al., Sediment source identification in a semiarid watershed at soil mapping unit scales, Catena (2011), doi:10.1016/j.catena.2011.05.002

Table 3
Selected physical and isotopic properties of soil mapping units in subwatershed 3.

Property	Units	Soil mapping units: Combate	Elgin–Stronghold	Luckyhills–McNeal	McAllister–Stronghold	Stronghold–Bernadino	Weighted mean	Suspended sediment
Sand	g kg^{-1}	685	756	720	697	739	720	374
Silt	g kg^{-1}	152	136	142	172	131	148	409
Clay	g kg^{-1}	163	108	138	131	130	133	216
WDC	g kg^{-1}	133	87	114	108	97	108	
AI		18.2	19.1	17.1	16.9	25.3	18.0	
δ^{13}C	‰	−19.10	−20.22	−21.43	−18.57	−18.27	−19.52	−22.72
C3 plants	%	41.6	49.4	57.9	37.8	35.7	44.5	67.0
C4 plants	%	58.4	50.6	42.1	62.2	64.3	55.5	33.0

The objective of the current study was to develop an approach to locate sediment sources in subwatersheds at soil mapping unit scales. This would be accomplished by using specific clay enrichment ratio data as indicators of sediment delivery in combination with a sediment yield index determined from measured aggregation index (erodibility) data weighted on the basis of relative area occupied by a given soil mapping unit.

2. Materials and methods

2.1. Site characteristics

As described in detail by Rhoton et al. (2008), this research was conducted in the Walnut Gulch Experimental Watershed (WGEW) of southeastern AZ (Fig. 1) to develop an approach for estimating the relative contributions of individual subwatersheds to the total suspended sediment load leaving the watershed. The WGEW, which encompasses the town of Tombstone (31°43′ N, 110°41′ W), contains approximately 150 km^2 in a high foothill alluvial fan portion of the larger San Pedro River watershed. Soil distribution in the WGEW (Fig. 1) is closely related to the parent materials (Rhoton et al., 2007) which are dominated by Quaternary alluvium from limestone (Alonso, 1997) that has weathered to well-drained, calcareous gravelly loam soils (Gelderman, 1970). The remaining watershed soils that were formed in alluvium and colluvium from andesite and basalt, and residuum from granodiorite, are generally finer textured, shallow, and well-drained. Rock and gravel contents on the soil surface range from 0 up to 70% on the very steep slopes (Simanton and Toy, 1994). The vegetation in WGEW is basically shrubs or grasses. The shrubs, which are primarily dominant in subwatersheds 3, 7, and 15, consist of creosote bush [*Larrea tridentate* (DC.) Coville], whitethorn (*Acacia constricta* Benth.), tarbush (*Flourensia cernua* DC.), snakeweed [*Gutierrezia sarothrae* (Pursh) Britton & Rusby], and burroweed [*Haplopappus tenuisectus* (Greene) S. F. Blake ex L. D. Benson]. The grass species of black grama [*Bouteloua eriopoda* (Torr.) Torr.], blue grama [*Bouteloua gracilis* (Kunth) Lag. Ex Griffi ths], side-oats grama [*Bouteloua curtipendula* (Michx.) Torr.], curly-mesquite [*Hilaria belangeri* (Steud.) Nash], and bush muhly (*Muhlenbergia*

Table 4
Selected physical and isotopic properties of soil mapping units in subwatershed 7.

Property	Units	Soil mapping units: Combate	Luckyhills	Luckyhills–McNeal	Mabray–Chiricahua–Rock	Mabray–Rock	Monterosa	Riverwash–Bodecker	Schiefflin	Sutherland–mule	Weighted mean	Suspended sediment
Sand	g kg^{-1}	869	739	693	641	662	648	847	790	755	719	498
Silt	g kg^{-1}	65	137	194	201	205	245	93	115	132	162	326
Clay	g kg^{-1}	65	124	113	159	132	107	60	95	114	118	175
WDC	g kg^{-1}	35	105	88	117	101	84	46	80	88	91	
AI		46.9	15.2	22.3	26.2	23.6	21.2	24.3	15.7	22.6	22.8	
δ^{13}C	‰	−21.26	−19.19	−21.99	−19.11	−21.17	−21.25	−21.92	−21.90	−20.28	−20.90	−23.03
C3 plants	%	56.8	42.2	61.9	41.6	56.1	56.7	61.4	61.3	49.8	54.2	69.2
C4 plants	%	43.2	57.8	38.1	58.4	43.9	43.3	38.6	38.7	50.2	45.8	30.8

Table 5
Selected physical and isotopic properties of soil mapping units in subwatershed 9.

Property	Units	Soil mapping units: Baboquivari–Combate	Elgin–Stronghold	Epitaph	Graham	Graham–Lampshire	Lampshire–Rock	Luckyhills–McNeal	McAllister–Stronghold	Stronghold–Bernadino	Tombstone	Weighted mean	Suspended sediment
Sand	g kg^{-1}	724	721	710	450	426	637	662	742	661	699	653	506
Silt	g kg^{-1}	159	130	176	334	366	139	208	105	112	169	184	337
Clay	g kg^{-1}	117	149	114	215	207	223	130	153	227	131	163	156
WDC	g kg^{-1}	82	105	71	136	115	184	82	102	157	90	111	
AI		29.4	30.3	38.0	34.2	44.5	20.1	37.0	33.2	30.4	32.0	31.9	
δ^{13}C	‰	−18.74	−17.73	−18.78	−16.92	−17.38	−19.63	−19.30	−16.40	−16.69	−19.15	−18.09	−20.51
C3 plants	%	39.0	31.9	39.3	26.2	29.4	45.3	43.0	22.5	24.6	41.9	34.3	51.5
C4 plants	%	61.0	68.1	60.7	73.8	70.6	54.7	57.0	77.5	75.4	58.1	65.7	48.5

Table 6
Selected physical and isotopic properties of soil mapping units in subwatershed 10.

Property	Units	Soil mapping units: Baboquivari–Combate	Blacktail	Budlamp–Woodcutter	Elgin–Stronghold	Epitaph	Forrest–Bonita	Graham	McAllister–Stronghold	Stronghold–Bernadino	Tombstone	Woodcutter	Weighted mean	Suspended sediment
Sand	g kg^{-1}	822	586	783	722	336	667	419	782	725	741	723	698	419
Silt	g kg^{-1}	98	152	129	137	406	206	291	95	133	139	131	142	410
Clay	g kg^{-1}	81	263	89	141	258	127	290	123	141	119	146	160	171
WDC	g kg^{-1}	51	206	59	92	73	95	196	93	106	90	109	116	
AI		33.8	22.0	33.5	35.0	71.6	25.9	32.5	24.1	24.8	24.7	27.9	28.1	
δ^{13}C	‰	−18.98	−18.04	−19.44	−17.56	−18.07	−18.31	−16.71	−19.45	−17.85	−20.47	−18.16	−18.24	−20.57
C3 plants	%	40.7	34.1	43.9	30.7	34.3	36.0	24.7	44.0	32.7	51.2	35.0	35.5	51.9
C4 plants	%	59.3	65.9	56.1	69.3	65.7	64.0	75.3	56.0	67.3	48.8	65.0	64.5	48.1

porteri Scribn. ex Beal) are the dominant vegetation in subwatersheds 9, 10, and 11 (Simanton et al., 1994). Land-use in the watershed is rangeland.

2.2. Study approach

Suspended sediments were collected using vertical samplers mounted near the center of supercritical flumes (Renard et al., 1993) in SWs 3, 7, 9, 10, 11, and 15. The suspended samples flowed through 6.4 mm diameter ports drilled into the 10.2-cm diameter (i.d.) aluminum tube body of the sampler at 30.5 cm increments of flow. Plastic tubing connected the ports to 500-mL plastic sample bottles mounted at each depth increment inside the sealed sampler. Suspended samples collected over an eight year period by this method were analyzed by year, and averaged to give one overall value per flume.

Soil samples were collected from the subwatersheds based on relative acreage occupied by individual mapping units (Rhoton et al., 2008). The process consisted of superimposing the digitized soil survey (1:5000) on the digital elevation model (DEM) for each subwatershed. A sampling transect length of 1000 m for each 200 ha of a given soil mapping unit (Fig. 2) was delineated on the DEM using geographic positioning system derived coordinates. Three separate samples were collected 10 m apart from the surface 5.0 cm at each sampling location along the transect, and composited to form a single sample. Site data were recorded for latitude–longitude, slope position, slope steepness, and slope aspect.

2.3. Laboratory analysis

In the laboratory, all soil and sediment samples were air-dried or oven-dried at 60 °C and sieved to <2 mm. Particle size distribution was determined by standard pipette analysis following overnight dispersion in Na hexametaphosphate (NRCS, 1996). The water-dispersible clay (WDC) component of the total clay fraction was also estimated by this methodology, using only distilled water as the dispersant. The total clay and WDC content data were used to calculate an aggregation index (AI) for the watershed soils based on the method of Harris (1971) as follows: $AI = 100\ (1 - WDC/total\ clay)$. These AI data were used to calculate a potential sediment yield index (PSYI) for the major soil mapping units in each of the six subwatersheds. This index was derived by multiplying the percent relative area occupied by each soil mapping unit in a given subwatershed times $(100 - AI)$. The results from this calculation were then summed for all the soil mapping units to obtain the sediment yield index for a specific subwatershed based on their erodibility and relative area.

The δ^{13}C was determined by the Stable Isotope Lab at the University of California-Davis using a PDZ Europa mass spectrometer (Northwich, UK). As a pretreatment for stable carbon isotope analysis, carbonate carbon was removed by shaking all samples in a 10% acetic acid solution until effervescence ceased. The samples were then washed three times in distilled water and centrifuged after each washing. Procedural details were identical to those reported elsewhere (Biedenbender et al., 2004; Bekele and Hudnall, 2003). The relative contributions of C3 and C4 plants to δ^{13}C were estimated by the mass balance equation of Boutton (1996) as follows:

$$x = \delta^{13}C_{soil,sediment} - \delta^{13}C_{C3} / \delta^{13}C_{C4} - \delta^{13}C_{C3}$$

where x is the relative amount of carbon derived from C4 plants, $\delta^{13}C_{soil,\ sediment}$ is the δ^{13}C of the soil and sediment organic fractions, $\delta^{13}C_{C4}$ is the average δ^{13}C value of the C4 plants (−13‰), and $\delta^{13}C_{C3}$ is the average δ^{13}C value of C3 plants (−27‰). The relative amount of carbon derived from C3 plants is $1 - x$.

Please cite this article as: Rhoton, F.E., et al., Sediment source identification in a semiarid watershed at soil mapping unit scales, Catena (2011), doi:10.1016/j.catena.2011.05.002

Table 7
Selected physical and isotopic properties of soil mapping units in subwatershed 11.

Property	Units	Soil mapping units					Weighted mean	Suspended sediment
		Baboquivari–Combate	Elgin–Stronghold	McAllister–Stronghold	Stronghold–Bernadino	Tombstone		
Sand	g kg^{-1}	710	735	696	748	705	731	512
Silt	g kg^{-1}	166	152	159	115	163	136	321
Clay	g kg^{-1}	124	114	145	137	132	133	168
WDC	g kg^{-1}	104	83	126	101	103	102	
AI		16.0	27.0	13.4	26.2	21.9	23.9	
δ^{13}C	‰	−17.32	−17.41	−17.37	−17.19	−19.19	−17.70	−20.76
C3 plants	%	29.0	29.6	29.4	28.1	42.2	31.7	53.2
C4 plants	%	71.0	70.4	70.6	71.9	57.8	68.3	46.8

All statistical analysis related to soil and sediment properties used the GLM and CORR procedures of SAS Version 8 (SAS Institute, 1999).

3. Results and discussion

3.1. Watershed soil and sediment characteristics

Taxonomic criteria for the soil mapping units and their associated landforms (Table 1) indicate that aridisols, developed on fan remnants and hills, are the predominant soils in the WGEW (Breckenfeld et al., 1995). The parent materials, consisting of alluvium and erosion products from igneous, metamorphic, and carbonate rocks, differ substantially among subwatersheds (Fig. 1). The 4300 ha mapped as the Luckyhills–McNeal complex represent the most widely distributed soils in the watershed (Table 2). The Elgin–Stronghold, McAllister–Stronghold, Mabray–Chiricahua, and Tombstone were the only other mapping units with significant acreage. The physical and chemical, and isotopic properties of the surface soils, and their associated suspended sediments collected at the outlet of each subwatershed are shown in Tables 3–8. The mean values listed for a given soil property represent a weighted average that is based on the relative acreage occupied by a given soil mapping unit.

Particle size data indicate that the suspended sediments were finer than the watershed soils, with the exception of subwatershed 9 (Tables 3–8), which indicates selective erosion and transport of the silt and clay fractions. Relative to the watershed soils, clay enrichment ratios (ER) of the suspended sediment in the six subwatersheds (Table 9) ranged from 0.96 to 1.62. The two subwatersheds (3, 7) with the greatest ER also had the lowest AI values of 18.0 and 22.8, respectively. Conversely, subwatershed 9 had the highest AI value (31.9) which resulted in sediment depleted in clay relative to its soils. The clay ER of 0.96 for this subwatershed was the lowest recorded for the study. Thus, subwatersheds 3 and 7 had the most highly erodible soils in the WGEW, and subwatershed 9 had the least erodible. The correlation coefficient (r) determined for the clay ER of suspended sediments versus AI values for the subwatershed soils was −0.946 ($P \leq 0.01$). These results clearly indicate that AI can be used to accurately assess the erodibility of these soils.

As discussed in detail elsewhere (Rhoton et al., 2006; 2007; 2008), most of the other suspended sediment properties were also enriched relative to the watershed soils. An exception was the depletion of the % C4 plant (grasses) versus % C3 plant (shrubs) contribution to the stable C isotope component of the suspended sediments relative to the soils in all subwatersheds (Tables 3–8).The C4 fraction was greatest in the soils from subwatersheds 11 (68.3%), 9 (65.7%), and 10 (64.5%) due to predominately grassland vegetation. Subwatershed 7 soils had the lowest % C4 component at 45.8%. The soils from subwatersheds 3 and 15 were intermediate at 55.5 and 57.6%, respectively.

The relative percentage of C3 plant (shrub) contributions to the stable C isotopes in the soils were greatest in subwatersheds 7 (54.2%), 3 (44.5%), and 15 (42.4%) due to a predominance of shrub vegetation. The ratios of C3/C4 plant percentages in the stable C isotopes for the soil and sediment samples (Table 9) increased substantially in the sediment. The absolute differences in C3/C4 ratios (sediment minus soil) in subwatersheds 3, 7, and 11 were 1.23, 1.07, and 0.68, respectively. The differences for subwatersheds 9, 10, and 15 were more similar at 0.54, 0.53, and 0.59, respectively.

These absolute differences (increases) in C3/C4 plant ratios from watershed soils to suspended sediments are essentially another indicator of relative soil erodibility for these soils since they correlate so well with their respective AI and clay ER values. More specifically, since the relative percentage of the C3 plant component of the stable C isotope is greatest in the sediment from the sparsely vegetated soils in shrub-dominated subwatersheds (3, 7, 11, and 15 to a lesser extent), which also have the highest clay ER and lowest AI values, it is an indication of enhanced erosion due to more highly erodible soils. Conversely, in subwatersheds 9 and 10 where grass is the predominant vegetation, there is lower soil erodibility, less erosion, and a relatively lower percentage of C4 plant derived stable C isotopes in the suspended sediments as a result of greater vegetative soil cover afforded by the grass, and the higher AI values.

3.2. Sediment source tracking

The AI data for each soil mapping unit were used with its percent acreage in each subwatershed to calculate a potential sediment yield index (Table 10). The individual PSYI values were then summed for a weighted subwatershed value. This process is shown conceptually using the data from subwatershed 11 (Fig. 3). Relative to contributions from individual soil mapping units in the WGEW, the PSYI values indicate that most of the sediment originates in the Luckyhills–McNeal, Elgin–Stronghold, McAllister–Stronghold, Stronghold–Bernardino, and Tombstone mapping units. These soils were formed on a range of parent materials, and vary considerably relative to acreage among subwatersheds, but all are generally characterized by coarse textures, and relatively low organic carbon contents that contribute to the lower AI values in the WGEW. Subwatershed 3 consists almost entirely of these first four mapping units (Table 3) with AI values that range from 16.9 (McAllister–Stronghold) to 25.3 (Stronghold–Bernardino). Based on the PSYI values, the Luckyhills–McNeal (39.4) and the McAllister–Stronghold (24.1) mapping units contribute approximately 78% of the suspended sediment in this subwatershed, and the Elgin–Stronghold and Stronghold–Bernardino account for the remaining 22%.

Along with the highly erodible Luckyhills–McNeal mapping unit, the Mabray and Schiefflin soils account for approximately 90% of the PSYI in subwatershed 7. These soils formed on detritus from igneous and carbonate rocks, and are similar to the soils in subwatershed 3 with respect to low clay contents. In fact, the Schiefflin soil contained only 95 g kg^{-1} clay which is the lowest concentration recorded for the major soils in the WGEW. The low clay and organic carbon contents

Table 8
Selected physical and isotopic properties of soil mapping units in subwatershed 15.

Property	Units	Soil mapping units														
		Combate	Epitaph	Forrest–Bonita	Graham	Graham–Lampshire	Grizzle	Luckyhills–McNeal	Mabray–Rock	Chiricahua–Mabray–Rock	McAllister–Stronghold	Monterosa	Sutherland	Tombstone	Weighted mean	Suspended sediment
Sand	$g\ kg^{-1}$	651	569	539	347	445	718	706	528	438	694	516	608	717	608	423
Silt	$g\ kg^{-1}$	238	255	292	467	335	181	183	281	431	175	342	267	154	251	395
Clay	$g\ kg^{-1}$	111	176	169	185	219	101	111	191	131	131	142	125	129	141	182
WDC	$g\ kg^{-1}$	83	127	126	99	120	70	80	125	104	96	107	97	99	98	
AI		24.6	23.7	25.0	47.1	44.1	30.1	27.8	35.1	21.2	26.6	25.5	22.4	22.3	28.2	
$\delta^{13}C$	‰	−21.45	−17.79	−16.27	−18.66	−19.22	−21.31	−19.77	−20.30	−17.35	−19.15	−19.87	−19.03	−19.77	−19.23	−21.31
C3 plants	%	58.1	32.3	21.6	38.4	42.4	57.1	46.3	50.0	29.2	41.9	47.0	41.0	46.2	42.4	57.1
C4 plants	%	41.9	67.7	78.4	61.6	57.6	42.9	53.7	50.0	70.8	58.1	53.0	59.0	53.8	57.6	42.9

Table 9
Comparison of potential sediment yield index (PSYI) values with sediment clay enrichment ratios (ER), C3/C4 plant ratios, and mixing model estimations of sediment sources by subwatershed.

Subwatershed	PSYI	Clay ER	C3/C4 plant ratios			Mixing model estimates
			Soil	Sediment	Difference	
						%
3	81.7	1.62	0.8	2.03	+1.23	46
7	77.4	1.48	1.18	2.25	+1.07	22
9	68	0.96	0.52	1.06	+0.54	4
10	71.2	1.17	0.55	1.08	+.053	6
11	76	1.26	0.46	1.14	+0.68	4
15	72.9	1.29	0.74	1.33	+.059	18

Correlation coefficients (r)

PSYI versus Clay ER, 0.962**
PSYI versus C3/C4 ratio differences, 0.905**
PSYI versus Mixing model estimates, 0.816*

* Significant at the 0.05 probability level.
** Significant at the 0.01 probability level.

($59\ g\,kg^{-1}$) explain why the Schiefflin soil has one of the lowest AI values in the study. The AI values ranged from 15.2 (Luckyhills) to 46.9 (Combate), however, these two soils were mapped on only 2% of the subwatershed.

In subwatershed 9, the AI values ranged from 20.1 (Graham–Lampshire–Rock) to 44.5 (Graham–Lampshire). The Elgin–Stronghold mapping unit made up 38% of the PSYI in this subwatershed by virtue of its relatively large acreage (37.2%). When combined with the Tombstone and McAllister–Stronghold, these soils comprise 72% of the PSYI in this subwatershed, the largest in the WGEW. This subwatershed also contains some soils (Epitaph, Graham, Lampshire) formed on sediment from volcanic rocks (Fig. 1) that produced higher clay contents and AI values, but their relatively low acreage in the watershed (17.7%) resulted in a contribution of only 11.4 to the total PSYI value of 68.

The Baboquivari, Blacktail, Elgin–Stronghold, McAllister–Stronghold, Stronghold–Bernardino, and Tombstone mapping units in subwatershed 10 were generally evenly distributed, comprising approximately 88.6% of the 1579 ha. The AI values ranged from 22.0 (Blacktail) to 35.0 (Elgin–Stronghold), ignoring the unusually high 71.6 value from the Epitaph samples. This high AI probably came from the high clay content B-horizon. These individual PSYI values indicate that the sediment yield order is Blacktail>Tombstone>Elgin–Stronghold>McAllister–Stronghold>Stronghold–Bernardino>Baboquivari. The remaining soils contributed negligibly to the PSYI for this subwatershed which, at 71.2, was the second lowest in the WGEW.

Subwatershed 11 had the smallest acreage of the six subwatersheds in this study. As a result, the relatively large acreages of Stronghold–Bernardino (53.3%) and Tombstone (28.4%) soils are dominant, yielding PSYI values of 39.3 and 22.2, respectively. Thus, based on the total PSYI value, 81% of the sediment from subwatershed 11 should originate in the Stronghold–Bernardino and Tombstone mapping units. In subwatershed 15, the predominant soil mapping units are the Luckyhills–McNeal (31.3%), Sutherland (17.0%), and the Monterosa (10.5%). These soils account for 60% of the PSYI value of 72.9. Most of the remaining mapping units occur in generally similar acreages that sum to 41.2% of the subwatershed, and generally contribute equally to the remaining 40% of the PSYI value.

In terms of relative sediment yields expected from these subwatersheds, based on soil acreage and erodibility, the PSYI order is: 3 (81.7)>7 (77.4)>11 (76.0)>15 (72.9)>10 (71.6)>9 (68.0). In most cases, the absolute difference in PSYI values between individual subwatersheds is small due to the low soil AI values, and/or the relatively low acreage of soils that have a substantially higher AI. The largest difference was between subwatersheds 3 and 9, as previously

Please cite this article as: Rhoton, F.E., et al., Sediment source identification in a semiarid watershed at soil mapping unit scales, Catena (2011), doi:10.1016/j.catena.2011.05.002

Table 10
Potential sediment yield index values determined for individual soil mapping units by subwatershed.

Subwatershed	Soil mapping unit	Percent of watershed	Aggregation index	Potential sediment yield index
3	Combate	0.3	18.23	0.25
	Elgin–Stronghold	13.0	19.06	10.52
	Luckyhills–McNeal	47.0	16.23	39.37
	McAllister–Stronghold	29.0	16.93	24.09
	Stronghold–Bernadino	10.0	25.32	7.47
			Sum	81.70
7	Combate	0.8	46.93	0.42
	Luckyhills	1.3	15.24	1.10
	Luckyhills–McNeal	26.6	22.29	20.67
	Mabray–Chiricahua–Rock Outcrop	27.5	26.22	20.29
	Mabray–Rock Outcrop	17.9	23.65	13.67
	Monterosa	1.4	21.15	1.10
	Riverwash–Bodecker	0.8	24.28	0.61
	Schiefflin	17.6	15.69	14.84
	Sutherland	6.1	22.59	4.72
			Sum	77.42
9	Baboquivari	7.9	29.40	5.58
	Elgin–Stronghold	37.2	30.10	26.00
	Epitaph	3.0	38.00	1.86
	Graham	7.4	34.18	4.87
	Graham–Lampshire	5.1	44.47	2.83
	Graham–Lampshire–Rock Outcrop	2.2	20.13	1.76
	Luckyhills–McNeal	1.9	37.03	1.20
	McAllister–Stronghold	13.3	33.16	8.89
	Stronghold–Bernadino	1.6	30.14	1.11
	Tombstone	20.4	32.00	13.87
			Sum	67.97
10	Baboquivari	12.2	33.79	8.08
	Blacktail	15.8	21.97	12.33
	Budlamp–Woodcutter	4.1	33.51	2.73
	Elgin–Stronghold	18.2	34.95	11.84
	Epitaph	1.2	71.57	0.34
	Forrest–Bonita	1.2	25.88	0.89
	Graham	0.9	32.50	0.61
	McAllister–Stronghold	14.7	24.11	11.16
	Stronghold–Bernadino	11.5	24.80	8.65
	Tombstone	16.2	24.75	12.19
	Woodcutter	4.0	30.96	2.76
			Sum	71.58
11	Baboquivari	0.9	16.00	0.76
	Elgin–Stronghold	9.6	27.00	7.01
	McAllister–Stronghold	7.8	13.37	6.76
	Stronghold–Bernadino	53.3	26.22	39.22
	Tombstone	28.4	21.90	22.18
			Sum	76.03
15	Combate	2.5	24.62	1.88
	Epitaph	6.4	23.71	4.88
	Forrest–Bonita	4.3	25.02	3.22
	Graham	2.8	44.11	1.56
	Graham–Lampshire	4.8	47.06	2.54
	Grizzle	3.4	30.09	2.38
	Luckyhills–McNeal	31.3	27.84	22.59
	Mabray–Chiricahua–Rock Outcrop	1.5	35.14	0.97
	Mabray–Rock Outcrop	6.3	21.22	4.96
	McAllister–Stronghold	6.1	26.60	4.48
	Monterosa	10.5	25.51	7.82
	Sutherland	17.0	22.44	13.22
	Tombstone	3.1	22.26	2.41
			Sum	72.91

indicated, where the AI values were 18.0 and 31.9, respectively. Although the greater emphasis is on the PSYI values for individual soil mapping units in a given subwatershed, some comparison is warranted between PSYI summations in each, and the relative contribution of individual subwatersheds to the sediment load leaving the WGEW as predicted from previous mixing model results (Rhoton et al., 2008). The order of these estimated contributions shown in Table 9 ($3>7>15>10>11=9$) is reasonably similar to the ordering for PSYI. Seemingly, there are discrepancies in the PSYI values when compared to the mixing model results for the same subwatershed. For example, the relatively large PSYI value for subwatershed 11 is attributed to its high acreage of low AI, highly erodible soils. In terms of its predicted low contributions to the sediment load at the WGEW outlet, 11 has the smallest land area, and is located at the greatest distance from the watershed outlet. When subwatershed 11 values are removed, the subwatershed ordering of PSYI and mixing model predictions are identical. Thus, the PSYI values calculated for the individual subwatersheds do not necessarily translate directly to the mixing model results predicted at the WGEW outlet, because these predictions did not account for differences in distance from the outlet, number of rainfall and runoff events during the monitoring period, total discharge, slope factors, and type of erosion between the six

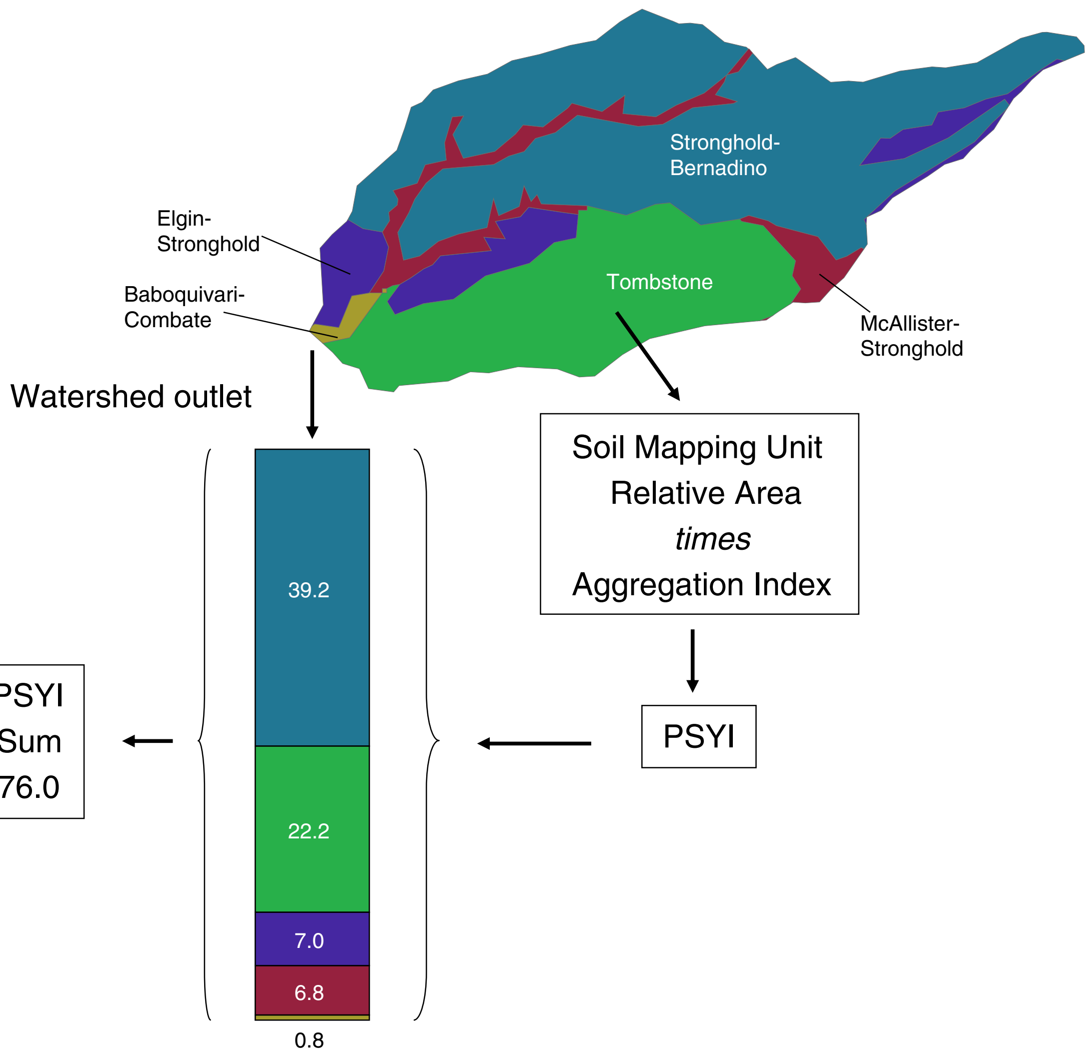

Fig. 3. Conceptual model illustrating the derivation of potential sediment yield index (PSYI) values using subwatershed 11 data from the Walnut Gulch Experimental Watershed as an example.

subwatersheds. Nevertheless, with subwatershed 11 data included, the correlation coefficient (r) determined for PSYI versus reported mixing model results was 0.816 ($P \leq 0.05$).

Interestingly, the subwatershed order for the clay ER was identical to the order for PSYI: 3>7>11>15>10>9. The correlation coefficient for PSYI versus clay ER (Table 9) was 0.962 ($P \leq 0.01$). Clearly, this parameter, which is an indicator of watershed soil erodibility, is also a good predictor of potential sediment yield at subwatershed scales. This result has implications for understanding the mechanisms associated with sediment enrichment ratios for this environment, and runs somewhat counter to assumptions previously reported and discussed in the scientific literature (e.g., Walling, 1983; Di Stefano and Ferro, 2002). In this environment, soil erodibility clearly appears to control the amount of clay enrichment of sediment being delivered from the subwatersheds, rather than preferential deposition of coarse materials during transport, and soil erodibility appears to control the total amount of sediment delivered from subwatersheds, rather than sediment delivery ratio.

Further, previous research (Ritchie et al., 2009; Rhoton et al., 2008) has shown that 63.8% of the stable C isotopes in the suspended sediment at the WGEW outlet are from C3 plant (shrubs) origin, and that the shrub-dominated subwatersheds (3, 7, and 15) contributed 86% of the suspended sediment leaving the WGEW. These three subwatersheds had less vegetation and lower clay contents relative to the C4 plant (grass)-dominated subwatersheds (9, 10, and 11), suggesting a strong relationship between stable carbon isotope composition, land cover, and erosion. The PSYI data in this study show similar trends. Specifically, the correlation coefficient for PSYI versus the C3/C4 plant ratio differences (Table 9) between soil and sediment was 0.905 ($P \leq 0.01$). Again, greater absolute differences in C3/C4 ratios translate into greater erodibility and PSYI.

4. Conclusions

The results from this research demonstrate that using aggregation index (AI), as an indicator of soil erodiblility, in combination with relative acreage occupied by individual soils within a watershed, to calculate a potential sediment yield index (PSYI), provides a reasonably accurate, simplified method for determining sediment sources at soil mapping unit scales. The PSYI values determined for the major soil mapping units in six subwatersheds are reasonably similar to mixing model results from a previous study (Rhoton et al., 2008) in addition to clay enrichment ratios, and the differences in the ratio of stable carbon isotopes from C3 plants (shrubs) versus C4 plants (grasses) between soils and suspended sediments. The apparent accuracy of this approach is linked to the soil sampling scheme used to determine aggregation index (erodibility), as samples were collected from all representative slope positions, slope gradients, and slope aspects in each mapping unit. Also, the suspended sediments reflect the contributions of all forms of soil erosion including rill, interrill, sheet, and gully.

Although this approach works for semiarid rangeland soils with relatively low aggregation indices (high erodibility) and sparse vegetative cover, the inclusion of a management factor will likely be necessary in higher rainfall regions with multiple land-uses.

Our results, with respect to ER being positively correlated to sediment delivery indicate that in this environment, soil erodibility at the source may control the degree of clay enrichment rather than preferential deposition of coarse materials during transport. The positive correlation between ER and PSYI (AI multiplied by watershed soil area) indicates that soil erodibility controls sediment delivery amounts rather than sediment delivery ratio.

A potential shortcoming of this PSYI approach to sediment source identification is the lack of accounting for streambank and channel contributions to the suspended sediment collected at the subwatershed flumes. However, since there is such good agreement between soil and sediment properties that can be attributed to preferential erosion and sediment transport we believe that the primary source of the suspended sediment is the watershed soils. This is also supported by the knowledge that significant channel lengths in all subwatersheds have no streambanks. Instead, the channels exist in gently sloping swales that funnel all runoff into the streams. Additionally, since large reaches of the streambanks in the Walnut Gulch Experimental Watershed are composed of caliche and/or bedrock, minimal contributions to the finer suspended sediment fractions can be expected from the streambanks.

Finally, the identification of sediment sources at soil mapping unit scales is important for several reasons. Previously, sediment source estimations in the Walnut Gulch Experimental Watershed were limited to subwatershed scales as large as 2400 ha. The calculation of PSYI values, as described, accurately identifies which soil mapping unit should yield the greatest amount of runoff and sediment for a given rainfall event. Further, under the conditions of a single soil mapping unit the PSYI can be determined at slope class or slope position scales within the mapping unit. Thus, we can delineate relatively small source areas (<50 ha) in watersheds, or fields that contribute the greatest amounts of sediment and associated pollutants, and require implementation of site specific BMPs to most efficiently reduce pollutant loadings to acceptable levels. Using this PSYI approach, we can eliminate the need for most labor intensive analytical procedures, and mixing model predictions. Lastly, this approach will make it possible to assign sediment credits to individual farms in a watershed, and assess the effectiveness of remediation efforts designed to reduce sediment loadings.

References

Alonso, M.A., 1997. Controls on erosion, sub-basins of Walnut Gulch, Arizona. In: Wang, S., et al. (Ed.), Proc. Conf. on Management of Landscapes disturbed by Channel Incision, Oxford, MS. 19–23 May1996. : Ctr. For Computational Hydrosci. and Eng. Univ. of Mississippi, Oxford, pp. 861–866.

Avnimelech, Y., McHenry, J.R., 1984. Enrichment of transported sediments with organic carbon, nutrients, and clay. Soil Sci. Soc. Am. J. 48, 259–266.

Bekele, G., Hudnall, W.H., 2003. Stable carbon isotope study of the prairie-forest transition soil in Louisiana. Soil Sci. 168, 783–792.

Biedenbender, S.H., McClaran, M.P., Quade, J., Weltz, M.A., 2004. Landscape patterns of vegetation change indicated by soil carbon isotope composition. Geoderma 119, 69–83.

Boardman, J., 1998. An average soil erosion rate for Europe: myth or reality? J. Soil Water Conserv. 53, 46–50.

Boutton, T.W., 1996. Stable carbon isotopes of soil organic matter and their use in documenting vegetation change in a savanna ecosystem. Geoderma 82, 5–41.

Breckenfeld, D.J., Svetlik, W.A., McGuire, C.E., 1995. Soil survey of Walnut Gulch Experimental Watershed. U.S. Gov. Print, Office, Washington, DC.

Brown, L.R., Wolf, E., 1984. Soil Erosion: Quiet Crisis in the World Economy. Worldwatch Paper 60. Worldwatch Institute, Washington, DC.

Caitcheon, C.G., 1998. The significance of various sediment magnetic mineral fractions for tracing sediment sources in Killimicat Creek. Catena 32, 131–142.

Dearing, J.A., Morton, R.A., Price, T.W., Foster, I.D.L., 1986. Tracing movement of topsoil by magnetic measurements: two case studies. Phys. Earth Planet. Inter. 42, 93–104.

Di Stefano, C., Ferro, V., 2002. Linking clay enrichment and sediment delivery processes. Biosyst. Eng. 81, 465–479.

Gelderman, F.W., 1970. Soil Survey: Walnut Gulch Experimental Watershed. Arizona. USDA-SCS Spec. Rep. U.S. Gov. Print. Office, Washington, DC.

Harris, S., 1971. Index of structure: evaluation of a modified method of determining aggregate stability. Geoderma 6, 155–162.

NRCS, 1996. Soil survey laboratory methods manual. Soil Surv. Invest. Rep., vol. 42. U.S. Gov. Print. Office, Washington, DC.

Oldfield, F., Rummery, T.A., Thompson, R., Walling, D.E., 1979. Identification of suspended sediment sources by means of magnetic measurements: some preliminary results. Water Resour. Res. 15, 211–218.

Ongley, E.D., 1982. Influence of season, source and distance on physical and chemical properties of suspended sediment. Recent Developments in the Explanation and Prediction of Erosion and Sediment Yield: IAHS Publ., 137, pp. 371–383.

Peart, M.R., Walling, D.E., 1988. Techniques for establishing suspended sediment sources in two drainage basins in Devon. UK: A comparative assessment: IAHS Publ., 174, pp. 269–279.

Pimentel, D.P., Harvey, C., Resosudarmo, K., Sinclair, K., Kurz, D., McNair, S., Crist, S., Shpritz, L., Fitton, L., Saffouri, R., Blair, R., 1995. Environmental and economic costs of soil erosion and conservation benefits. Science 267, 1117–1123.

Pimentel, D.P., 2000. Soil erosion and the threat to food security and the environment. Ecosyst. Health 6, 221–226.

Renard, K.G., Lane, L.J., Simanton, J.R., Emmerich, W.E., Stone, J.J., Weltz, M.A., Goodrich, D.C., Yakowitz, D.S., 1993. Agricultural impacts in an arid environment: Walnut Gulch studies. Hydrol. Sci. Technol. 9, 145–190.

Rhoton, F.E., Smeck, N.E., Wilding, L.P., 1979. Preferential clay mineral erosion from watersheds in the Maumee River Basin. J. Environ. Qual. 8, 547–550.

Rhoton, F.E., Emmerich, W.E., Goodrich, D.C., Miller, S.N., McChesney, D.S., 2006. Soil geomorphological characteristics of a semiarid watershed: influence on carbon distribution and transport. Soil Sci. Soc. Am. J. 70, 1532–1540.

Rhoton, F.E., Emmerich, W.E., Goodrich, D.C., Miller, S.N., McChesney, D.S., 2007. An aggregation/erodibility index for soils in a semiarid watershed, southeastern Arizona. Soil Sci. Soc. Am. J. 71, 984–992.

Rhoton, F.E., Emmerich, W.E., DiCarlo, D.A., McChesney, D.S., Nearing, M.A., Ritchie, J.C., 2008. Identification of suspended sediment sources using soil characteristics in a semiarid watershed. Soil Sci. Soc. Am J. 72, 1102–1112.

Rhoton, F.E., Bennett, S.J., 2009. Soil and sediment properties affecting the accumulation of mercury in a flood control reservoir. Catena 79, 39–48.

Ritchie, J.C., Nearing, M.A., Rhoton, F.E., 2009. Sediment budgets and source determinations using fallout Cesium-137 in a semiarid rangeland watershed, Arizona. USA. J. Environ. Radioact. 100, 637–643.

SAS Institute, 1999. The SAS system for windows. SAS Inst, Cary, NC.

Simanton, J.R., Toy, T.J., 1994. The relation between surface rock-fragment cover and semiarid hillslope profile morphology. Catena 23, 213–225.

Simanton, J.R., Renard, K.G., Christiansen, C.M., Lane, L.J., 1994. Spatial distributions of rock fragments along catenas in semiarid Arizona and Nevada, USA. Catena 23, 29–42.

Slattery, M.C., Burt, T.P., Walden, J., 1995. The application of mineral magnetic measurements to quantify within-storm variations in suspended sediment sources. IAHS Publ., 229, pp. 143–151.

Slattery, M.C., Burt, T.P., 1997. Particle size characteristics of suspended sediment in hillslope runoff and stream flow. Earth Surf. Processes Landforms 22, 705–719.

Sutherland, R.A., Bryan, R.B., 1989. Variability of particle size characteristic of sheetwash sediments and fluvial suspended sediment in a small semiarid catchment, Kenya. Catena 16, 189–204.

Trimble, S.W., Crosson, P., 2000. U. S. soil erosion rates: myth and reality? Science 289, 248–250.

Walling, D.E., 1983. The sediment delivery problem. J. Hydrol. 65, 209–237.

Walling, D.E., 2005. Tracing suspended sediment sources in catchments and river systems. Sci. Total Environ. 344, 159–184.

Walling, D.E., Moorehead, P.W., 1989. The particle size characteristics of fluvial suspended sediment. Hydrobiologia 176/177, 125–149.

Walling, D.E., Woodward, J.C., 1992. Use of radiometric fingerprints to derive information on suspended sediment source. IAHS Publ., No. 215, pp. 153–164.

Please cite this article as: Rhoton, F.E., et al., Sediment source identification in a semiarid watershed at soil mapping unit scales, Catena (2011), doi:10.1016/j.catena.2011.05.002